ChemComm

RSC Publishing

COMMUNICATION

View Article Online
View Journal | View Issue

Improvement of hydrothermal stability of zeolitic imidazolate frameworks†

Cite this: *Chem. Commun.*, 2013, **49**, 9140

Received 14th July 2013,
Accepted 6th August 2013

DOI: 10.1039/c3cc45308a

www.rsc.org/chemcomm

Xinlei Liu,[ab] Yanshuo Li,*[a] Yujie Ban,[ab] Yuan Peng,[ab] Hua Jin,[ab] Helge Bux,[a] Longya Xu,[a] Jürgen Caro[c] and Weishen Yang*[a]

The metal–organic framework ZIF-8, which undergoes hydrolysis under hydrothermal conditions, is endowed with high water-resistance after a shell-ligand-exchange-reaction. The stabilized ZIF-8 retains its structural characteristics with improved application performances in adsorption and membrane separation.

Metal–organic frameworks (MOFs) or porous coordination polymers (PCPs) are an emerging class of nanoporous materials showing a wide range of potential applications, *e.g.* gas storage, molecular separation, chromatography, heterogeneous catalysis and smart sensoring.[1] Yet for most of the MOFs, one of the major drawbacks is their poor hydrothermal stability, which is clearly a limitation to their practical applications.[2] Development of novel MOF structures with high stability is an important research topic.[3,4] To date, only a few MOFs are reported to possess satisfactory hydrothermal stability, *e.g.* the ZIF (zeolitic imidazolate framework) family,[4] MIL (Matérial Institut Lavoisier) analogues[3b] and some zirconium[3c–e] and pyrazolate[3a] based MOFs. On the other hand, from a practical point of view, post-enhancement of hydrothermal stability of the already existing MOF materials is a more attractive option and one of the most active research domains nowadays.[5] However along with improved stability, the application properties of the parent MOFs were usually impaired, *e.g.* considerable decrease of the specific surface area (SSA) after different post-treatments.[5b–d]

In this study, the hydrothermal stability of ZIF-8, one prototypical member of the ZIF family, was intensively studied. ZIF-8 crystallizes with a sodalite (SOD)-related structure with a formula of Zn (2-methylimidazolate)$_2$.[4a,b] ZIF-8 has drawn extensive research interest from both academic[4] and industrial societies[2a] due to its exceptional thermal and chemical stability. In this work, however, we observed experimentally that ZIF-8 underwent hydrolysis under hydrothermal conditions, regardless of its size (nano- or micro-crystals, Fig. S1 and S2, ESI†) and origin (*e.g.* even the ZIF-8 synthesized in water showed instability after exhaustive washing, Fig. S3 and S4, ESI†). This is also found to be a general phenomenon for other types of ZIFs (Fig. S5 and S6, ESI†). The observed difference in ZIF's stability can be attributed to the careful elimination of the protective effect of released ligands in our stability tests (ESI†), which has never been noticed before.

Herein we report our strategy for improving the hydrothermal stability of ZIF-8 *via* a shell-ligand-exchange-reaction (SLER). A number of excellent advancements in ligand exchange of MOFs have been made in the very recent years.[6] Different from the above cases in most of which complete ligand exchange is desired and attempted, in the SLER employed here, the ligand exchange reaction mainly occurs in the outermost shell of ZIF-8 particles as shown in Scheme 1. After SLER, the ZIF-8 (termed ZIF-8–DMBIM) retained its original crystal structure and exhibited remarkably enhanced hydrothermal stability without sacrificing, or even improving, the application performances in adsorption and membrane separation. The optimized recipe for SLER is: DMBIM (5,6-dimethylbenzimidazole), methanol, triethylamine (TEA) and fresh ZIF-8 nanocrystals were dispersed in methanol in a glass bottle (weight composition: ZIF-8–DMBIM–TEA–MeOH = 1 : 1 : 0.7 : 160) and thereupon mixed. After being heated at 60 °C for 15 h, the product was washed with methanol for later use.

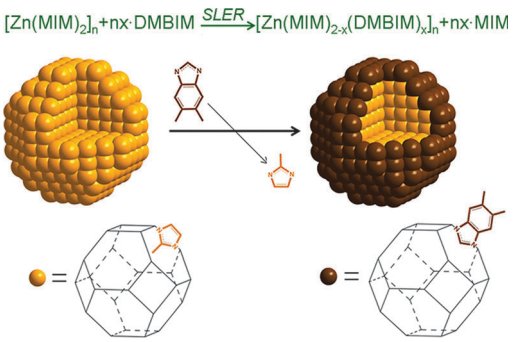

Scheme 1 Schematic representation of the shell-ligand-exchange-reaction (SLER) process of ZIF-8.

[a] *State Key Laboratory of Catalysis, Dalian Institute of Chemical Physics, CAS, Zhongshan Road 457, 116023, Dalian, China. E-mail: leeys@dicp.ac.cn, yangws@dicp.ac.cn*
[b] *University of Chinese Academy of Sciences, Beijing 100049, China*
[c] *Institute of Physical Chemistry and Electrochemistry, Leibniz University Hannover, Callinstrasse 3A, 30167, Hannover, Germany*

† Electronic supplementary information (ESI) available: Experimental and characterization details. See DOI: 10.1039/c3cc45308a

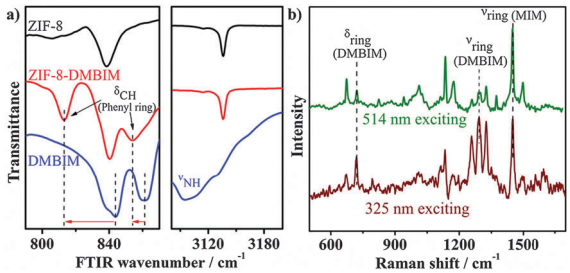

Fig. 1 (a) FTIR-ATR spectra of ZIF-8 (black), DMBIM (blue) and ZIF-8–DMBIM (red). (b) Raman spectra of ZIF-8–DMBIM using 325 nm (wine) and 514 nm (olive) exciting laser wavelength.

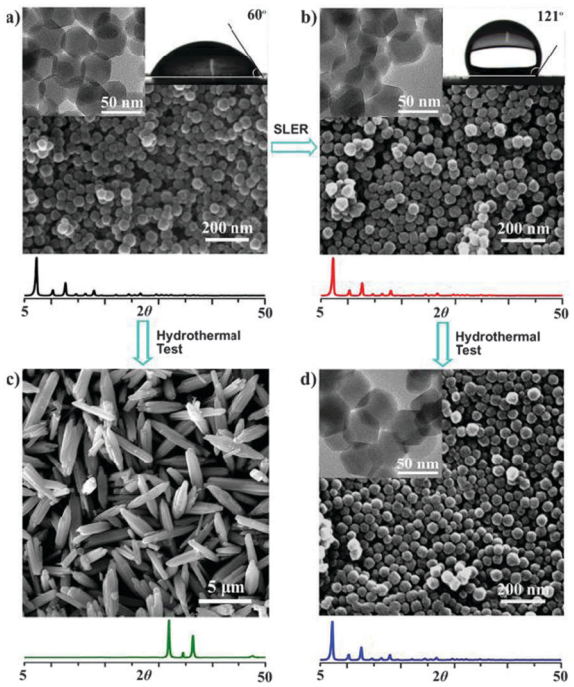

Fig. 2 SEM images and XRD patterns of (a) ZIF-8, (b) ZIF-8–DMBIM, (c) ZIF-8 after the hydrothermal test and (d) ZIF-8–DMBIM after the hydrothermal test. The insets are the corresponding TEM images and the contact angle images of water droplets.

The success of SLER was verified by FTIR-ATR and UV-vis Raman spectroscopy. As shown in the FTIR spectra of ZIF-8–DMBIM (Fig. 1a), two new peaks appeared at 813 cm^{-1} and 854 cm^{-1}, corresponding to the C–H out-of-plane deformation vibrations in the phenyl rings of DMBIM. A considerable red shift was observed compared with pure DMBIM, implying deprotonation of DMBIM and subsequent coordination of imidazole nitrogen to zinc ions. The disappearance of the broad band at 3100 cm^{-1} (N–H stretching vibrations) provides further evidence for the deprotonation–coordination process (Fig. S7 and S8, ESI†). UV-vis Raman spectroscopy, employing exciting laser with different wavelengths, is a powerful tool for studying the different compositions of the surface and bulk of a solid sample.[7] In the Raman spectra (Fig. 1b), the intensity of the in-plane deformation vibrations (720 cm^{-1}) and stretching vibrations (1293 cm^{-1}) originating from the fused rings of DMBIM decreases remarkably upon increasing the wavelength of the exciting laser (from 325 to 514 nm) compared with the ring-stretching vibrations originating from MIM (2-methylimidazolate, 1450 cm^{-1}). For this given material, the penetration depth is directly proportional to the exciting wavelength because of decreased absorbance (Fig. S9, ESI†). This signifies that the ligand exchange takes place mainly in the outermost layer of ZIF-8 nanoparticles (Fig. S10, ESI†). This might be because the bulky DMBIM is too big to pass through the narrow windows of ZIF-8 due to the molecular sieving effect. The ligand exchange molar ratio ($M_{DMBIM}/(M_{DMBIM} + M_{MIM})$) is 9.1%, as identified by ^{1}H NMR (Fig. S11, ESI†).

The structural integrity of ZIF-8–DMBIM after SLER treatment was evidenced by the unaltered powder X-ray diffraction (PXRD) patterns (Fig. 2a and b). The ZIF-8–DMBIM nanoparticles maintained a rhombic dodecahedron shape with a narrow size distribution of around 40 nm (Fig. 2a and b insets).

The hydrolysis-resistance abilities of ZIF-8 and ZIF-8–DMBIM were compared *via* hydrothermal tests in distilled water at 80 °C for 24 hours. A very small amount of crystals (18 mg of the sample immersed in 30 ml of water, 0.060 wt%) was used in order to exclude the protective effect of released ligands (Fig. S1–S4, ESI†). In contrast to the original ZIF-8 nanoparticles, which completely transformed into ZnO (Fig. 2c), the crystal structure and morphology of the ZIF-8–DMBIM nanoparticles remained essentially unchanged after the test (Fig. 2d). Water contact angle measurements were carried out to assess the changes in hydrophobicity after SLER treatment (Fig. 2a and b insets). The ZIF-8–DMBIM showed a significant increase in the contact angle of water (121°) compared with the original ZIF-8 (60°), which can be well explained by the effective introduction of hydrophobicity within the outermost layer of the ZIF-8 nanoparticles by DMBIM substitution. SLER with other kinds of imidazole derivatives was also attempted to enhance the hydrolysis-resistance of ZIF-8. Different degrees of enhancement were achieved depending on the physicochemical properties of the ligands (Fig. S12, ESI†).

The textural characteristics of ZIF-8 and ZIF-8–DMBIM were quantified by measuring the nitrogen sorption isotherms at 77 k. The isotherm curves (both adsorption and desorption branches) of ZIF-8–DMBIM are consistent with that of ZIF-8. Only a negligible decrease in BET surface area and pore volume was observed after SLER (Fig. S13 and S14, ESI†).

ZIF-8 has been proven to be very promising for the efficient recovery of bio-alcohols from aqueous solutions.[8] In this work, the isobutanol sorption isotherms of ZIF-8–DMBIM were collected on an Intelligent Gravimetric Analyzer (IGA). After SLER treatment, ZIF-8–DMBIM showed only a slight decrease in the equilibrium adsorption capacity at 3.5 kPa (Fig. 3a), which coincides with the results from BET. An interesting observation is the absence of the "gate opening" effect (hysteretic adsorption behaviour)[9] in the adsorption of isobutanol on ZIF-8–DMBIM. This is in contrast to ZIF-8, for which a threshold pressure ("gate-opening" pressure) of 0.5 kPa was observed for the uptake of isobutanol (Fig. 3a). As presented in Fig. 3b, although the DMBIM ligand is more bulky than MIM, the isobutanol transport diffusivity in ZIF-8 was obviously enhanced after SLER. These phenomena observed on ZIF-8–DMBIM might be a result of the specific framework–guest interaction.[9c] No doubt, the steep adsorption uptake of isobutanol at low pressure and the enhanced transport diffusivity are clearly of benefit for the applications in adsorption and membrane based separation.

The application performance of ZIF-8–DMBIM in liquid-phase adsorption was evaluated employing the solution-depletion method (ESI†) with the emphasis on its hydrothermal stability. In order to

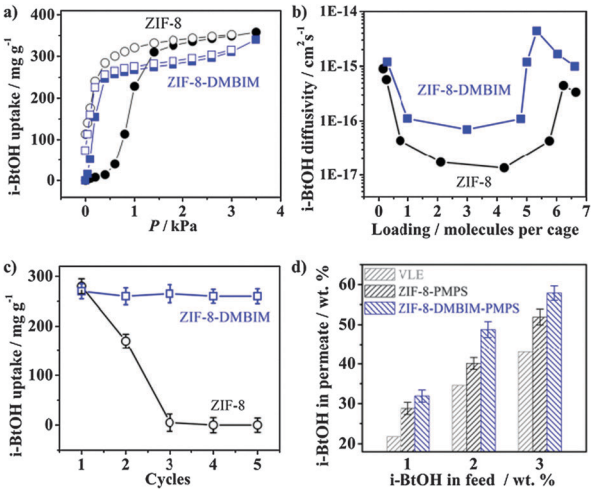

Fig. 3 (a) isobutanol (40 °C) sorption isotherms and (b) transport diffusivity on ZIF-8 (black circles) and ZIF-8–DMBIM (blue squares). Filled and open symbols represent the adsorption and desorption branches, respectively. (c) Uptake of isobutanol (3.0 wt%, 25 °C) on ZIF-8 (black) and ZIF-8–DMBIM (blue) over five cycles. (d) isobutanol concentration in the permeate (downstream side) at different feed concentrations (upstream side, at 80 °C) for ZIF-8 (black) and ZIF-8–DMBIM (blue) derived mixed matrix membranes (MMMs). Vapor–liquid equilibrium (VLE) data (gray) are also shown for comparison.

accelerate the evaluation process, the adsorbents were periodically treated under harsh conditions (0.060 wt% adsorbents in 3.0 wt% isobutanol solution at 80 °C for 24 h) after each adsorption–desorption cycle (ESI†). As shown in Fig. 3c, the uptake capacity of ZIF-8 decreased to around zero after 4 cycles due to the hydrolysis induced amorphization of the SOD structure (Fig. S15, ESI†). In contrast, no discernible degradation of the isobutanol uptake occurred on ZIF-8–DMBIM, thanks to its excellent hydrothermal stability (Fig. S15, ESI†).

In our previous studies, by dispersing ZIF-8 nanoparticles into silicone rubber (*e.g.* polymethylphenylsiloxane, PMPS), we got the so-called mixed-matrix-membranes (MMMs).[8a,10] In the current work, a ZIF-8–DMBIM–PMPS membrane was prepared and tested for pervaporation recovery of isobutanol from water (ESI†). When exposing the ZIF-8–DMBIM–PMPS membrane to a feed containing 3.0 wt% isobutanol, a permeate containing 58 ± 2wt% isobutanol was obtained. This value is *ca.* 1.40 ± 0.05 times higher than that obtained *via* evaporation which is determined by the vapor–liquid equilibrium (VLE). Compared with the ZIF-8–PMPS membrane, the ZIF-8–DMBIM–PMPS membrane exhibited improved selectivity towards isobutanol while keeping the isobutanol flux (productivity) constant (Fig. 3d, Fig. S16–S18, ESI†). This performance also ranks among the highest values for organophilic pervaporation membranes.[8a] The improved selectivity results from the increased hydrophobicity, the decreased threshold pressure for isobutanol adsorption and the enhanced transport diffusivity after SLER treatment of ZIF-8.

In summary, ZIF-8 is currently one of the most stable metal–organic frameworks.[2a,4a,c] Nevertheless, our experimental results provided compelling evidence that ZIF-8 will undergo hydrolysis under hydrothermal conditions, where transformation to ZnO will be thermodynamically preferred.[2a] The hydrothermal stability of ZIF-8 can be remarkably improved *via* shell-ligand-exchange-reaction (SLER), taking advantage of the hydrophobicity (water-repellent) effect and the steric hindrance effect of DMBIM. After SLER treatment, the ZIF-8–DMBIM retains the structural characteristics of ZIF-8 with improved application performances in adsorption and membrane separation. Besides ZIF-8, the SLER methodology was also successfully applied to stabilize other types of ZIFs, *e.g.* ZIF-7 (SOD topology, Zn (benzimidazolate)$_2$)[4a,b] and ZIF-93 (RHO topology, Zn(4-methylimidazolate-5-carbaldehyde)$_2$)[11] (Fig. S5 and S6, ESI†). The stabilized ZIF materials are expected to be suitable for various applications under aqueous conditions, such as adsorbents, membranes, and heterogeneous catalysts.

This work was supported by the National Science Fund (21176231, 21006101, 21276249 and 21361130018) and the DICP Independent Research Project (No. R201006). The authors thank Prof. Dr Baokun Huang and Dr Min Wang for their kind support in Raman spectra characterization and contact angle measurements, respectively.

Notes and references

1 H. C. Zhou, J. R. Long and O. M. Yaghi, *Chem. Rev.*, 2012, **112**, 673.
2 (*a*) J. J. Low, A. I. Benin, P. Jakubczak, J. F. Abrahamian, S. A. Faheem and R. R. Willis, *J. Am. Chem. Soc.*, 2009, **131**, 15834; (*b*) K. A. Cychosz and A. J. Matzger, *Langmuir*, 2010, **26**, 17198.
3 (*a*) V. Colombo, S. Galli, H. J. Choi, G. D. Han, A. Maspero, G. Palmisano, N. Masciocchi and J. R. Long, *Chem. Sci.*, 2011, **2**, 1311; (*b*) G. Férey, C. Mellot-Draznieks, C. Serre, F. Millange, J. Dutour, S. Surblé and I. Margiolaki, *Science*, 2005, **309**, 2040; (*c*) J. H. Cavka, S. Jakobsen, U. Olsbye, N. Guillou, C. Lamberti, S. Bordiga and K. P. Lillerud, *J. Am. Chem. Soc.*, 2008, **130**, 13850; (*d*) V. Guillerm, F. Ragon, M. Dan-Hardi, T. Devic, M. Vishnuvarthan, B. Campo, A. Vimont, G. Clet, Q. Yang, G. Maurin, G. Férey, A. Vittadini, S. Gross and C. Serre, *Angew. Chem., Int. Ed.*, 2012, **51**, 9267; (*e*) D. Feng, Z. Y. Gu, J. R. Li, H. L. Jiang, Z. Wei and H. C. Zhou, *Angew. Chem., Int. Ed.*, 2012, **51**, 10307; (*f*) T. Borjigin, F. Sun, J. Zhang, K. Cai, H. Ren and G. Zhu, *Chem. Commun.*, 2012, **48**, 7613.
4 (*a*) K. S. Park, Z. Ni, A. P. Côté, J. Y. Choi, R. Huang, F. J. Uribe-Romo, H. K. Chae, M. O'Keeffe and O. M. Yaghi, *Proc. Natl. Acad. Sci. U. S. A.*, 2006, **103**, 10186; (*b*) X. C. Huang, Y. Y. Lin, J. P. Zhang and X. M. Chen, *Angew. Chem., Int. Ed.*, 2006, **45**, 1557; (*c*) Y. Pan, Y. Liu, G. Zeng, L. Zhao and Z. Lai, *Chem. Commun.*, 2011, **47**, 2071.
5 (*a*) J. G. Nguyen and S. M. Cohen, *J. Am. Chem. Soc.*, 2010, **132**, 4560; (*b*) J. B. Decoste, G. W. Peterson, M. W. Smith, C. A. Stone and C. R. Willis, *J. Am. Chem. Soc.*, 2012, **134**, 1486; (*c*) S. J. Yang and C. R. Park, *Adv. Mater.*, 2012, **24**, 4010; (*d*) J. Yang, A. Grzech, F. M. Mulder and T. J. Dingemans, *Chem. Commun.*, 2011, **47**, 5244; (*e*) H. Jasuja, Y. Huang and K. S. Walton, *Langmuir*, 2012, **28**, 16874.
6 (*a*) M. Kondo, S. Furukawa, K. Hirai and S. Kitagawa, *Angew. Chem., Int. Ed.*, 2010, **49**, 5327; (*b*) B. J. Burnett, P. M. Barron, C. Hu and W. Choe, *J. Am. Chem. Soc.*, 2011, **133**, 9984; (*c*) M. Kim, J. F. Cahill, H. Fei, K. A. Prather and S. M. Cohen, *J. Am. Chem. Soc.*, 2012, **134**, 18082; (*d*) O. Karagiaridi, M. B. Lalonde, W. Bury, A. A. Sarjeant, O. K. Farha and J. T. Hupp, *J. Am. Chem. Soc.*, 2012, **134**, 18790; (*e*) N. Yanai and S. Granick, *Angew. Chem., Int. Ed.*, 2012, **51**, 5638.
7 M. Li, Z. Feng, G. Xiong, P. Ying, Q. Xin and C. Li, *J. Phys. Chem. B*, 2001, **105**, 8107.
8 (*a*) X. L. Liu, Y. S. Li, G. Q. Zhu, Y. J. Ban, L. Y. Xu and W. S. Yang, *Angew. Chem., Int. Ed.*, 2011, **50**, 10636; (*b*) J. C. S. Remi, T. Rémy, V. V. Hunskerken, S. van de Perre, T. Duerinck, M. Maes, D. D. Vos, E. Gobechiya, C. E. A. Kirschhock, G. V. Baron and J. F. M. Denayer, *ChemSusChem*, 2011, **4**, 1074.
9 (*a*) C. Gücüyener, J. van den Bergh, J. Gascon and F. Kapteijn, *J. Am. Chem. Soc.*, 2010, **132**, 17704; (*b*) D. Fairen-Jimenez, S. A. Moggach, M. T. Wharmby, P. A. Wright, S. Parsons and T. Düren, *J. Am. Chem. Soc.*, 2011, **133**, 8900; (*c*) N. Nijem, H. Wu, P. Canepa, A. Marti, K. J. Balkus, Jr., T. Thonhauser, J. Li and Y. J. Chabal, *J. Am. Chem. Soc.*, 2012, **134**, 15201.
10 X. Liu, H. Jin, Y. Li, H. Bux, Z. Hu, Y. Ban and W. Yang, *J. Membr. Sci.*, 2013, **428**, 498.
11 W. Morris, B. Leung, H. Furukawa, O. K. Yaghi, N. He, H. Hayashi, Y. Houndonougbo, M. Asta, B. B. Laird and O. M. Yaghi, *J. Am. Chem. Soc.*, 2010, **132**, 11006.

